LYMPHOID NEOPLASIA

One siRNA pool targeting the λ constant region stops λ light-chain production and causes terminal endoplasmic reticulum stress

Ping Zhou,[1] Xun Ma,[1] Lakshmanan Iyer,[2] Chakra Chaulagain,[1] and Raymond L. Comenzo[1,2]

[1]Tufts Medical Center, Boston, MA; and [2]Tufts University School of Medicine, Boston, MA

Key Points

- Immunoglobulin light-chain and antibody production by plasma cells is significantly reduced by siRNA for the light-chain constant region.
- In plasma cells making intact antibodies, knockdown of light chains can cause terminal ER stress because of unpaired heavy chains.

In systemic light-chain amyloidosis, λ light chains produced by clonal plasma cells cause organ damage and early death. In pursuit of novel therapy, we developed 1 pool of short interfering RNA (siRNA) targeting the constant region of λ light chains that substantially and promptly reduces λ-light-chain production and secretion by human plasma cells regardless of sequence diversity. In clones producing intact immunoglobulin G (IgG) λ antibodies (containing paired heavy and light chains), the secretion of intact antibodies is reduced, and all 3 branches of the unfolded protein response are activated by accumulation of unpaired IgG heavy chains in the endoplasmic reticulum (ER). Moreover, an ER stress response can then become terminal with effector caspase activity mediated in part by the transcription of the Bcl-2 homology 3 domain only family member NOXA. This pool of siRNA can be used to reduce pathological λ-light-chain production and cause apoptosis in human plasma cells making intact IgGλ antibodies. (*Blood*. 2014;123(22): 3440-3451)

Introduction

The immunoglobulin light chains in systemic light-chain amyloidosis (AL) have a κ-to-λ case rate of 1 to 4 and cause cardiac-related deaths in up to 25% of patients within months of diagnosis.[1,2] Current therapies for AL aim to reduce light-chain production and include steroids, alkylating agents, immunomodulatory drugs, and proteasome inhibitors.[3] Although responses are notable, incurability and early cardiac death are more the norm, and more effective therapies are needed.[4,5]

Although the unfolded protein response (UPR) is constitutively active in plasma cells,[6] and although the pairing of light and heavy chains is under strict intracellular quality control in the endoplasmic reticulum (ER),[7,8] we learned in initial experiments that variable region–targeted λ-light-chain knockdown could trigger a reactive UPR and a terminal ER stress response, whereas knockdown of immunoglobulin G (IgG) heavy-chain expression had no impact on cell growth or viability. We then hypothesized that λ-light-chain (IgL) production could be disrupted by short interfering RNA (siRNA) targeting consensus sequences in the *IgL* constant region (CR) messenger RNA (mRNA) with 1 siRNA pool. We now report that this pool, siRNA targeting the CR of λ light chains (si[$IGLC_{CR}$]), significantly reduces IgL production and secretion by human plasma cells without regard for unique variable region gene sequences, and that, in human plasma cells making intact antibodies, treatment with si[$IGLC_{CR}$] results in the intracellular retention of unpaired immunoglobulin heavy chains (IgH), the activation of the UPR, and upregulation of genes involved in ER stress signaling[9] that can cause NOXA-mediated mitochondrial depolarization and caspase-dependent apoptosis. In addition, si[$IGLC_{CR}$] treatment can substantially reduce *IgL* message and intracellular IgL in AL patient plasma cells producing monoclonal IgL and can also increase caspase 3/7 activity in clones making intact antibodies.

Materials and methods

Cells

ALMC1 and ALMC2 cells (gift of Diane Jelinek) were cultured as described.[10] MM.1S and MM.1R cells from American Type Culture Collection (Manassas, VA), and EJM and OPM-2 cells from the German Collection of Microorganisms and Cell Cultures (Braunschweig, Germany) were cultured as directed. These cell lines were chosen because they are human myeloma cell lines that produce λ light chains (IgL). Z-VAD-FMK, L-phenylalanine mustard, and arachadonic acid were from Sigma-Aldrich (St. Louis, MO).

Clinical specimens obtained under an institutional review board–approved protocol from patients with confirmed diagnosis of systemic AL and monoclonal IgL disease were used for CD138 selection as previously described.[11] This study was conducted in accordance with the Declaration of Helsinki.

IgL and *IgH* gene identification

Monoclonal *IgL* and *IgH* genes for ALMC1, ALMC2, and EJM cells were identified and sequenced as previously described.[12]

Submitted October 27, 2013; accepted March 27, 2014. Prepublished online as *Blood* First Edition paper, April 10, 2014; DOI 10.1182/blood-2013-10-535187.

P.Z. and X.M. contributed equally to this study.

The online version of this article contains a data supplement.

The publication costs of this article were defrayed in part by page charge payment. Therefore, and solely to indicate this fact, this article is hereby marked "advertisement" in accordance with 18 USC section 1734.

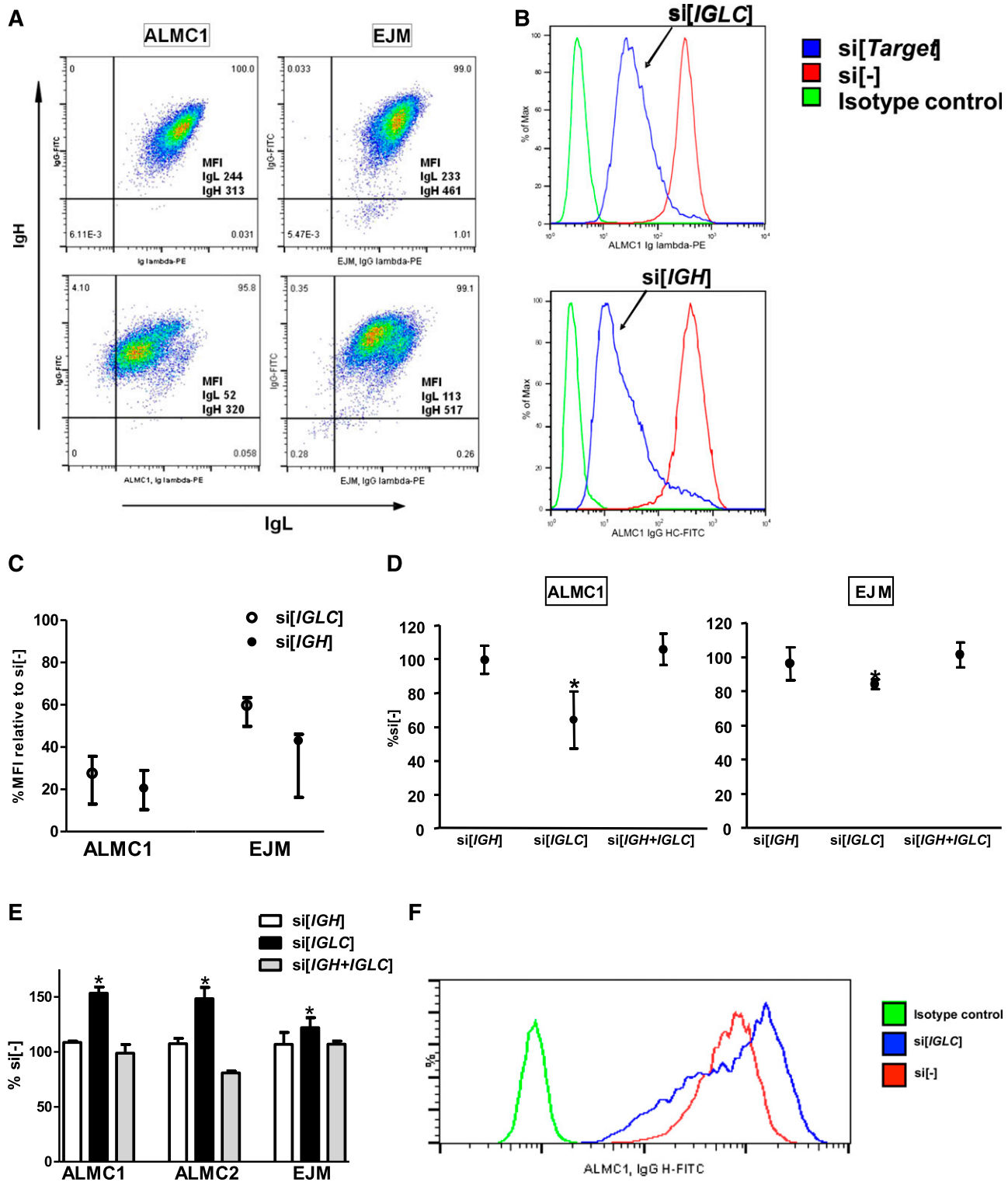

Figure 1. Plasma cell light and heavy chains can be knocked down with siRNA. (A) The flow cytometry plots in the upper row (si[-]) show that ALMC1 and EJM cells both produce intact IgGλ immunoglobulins but that EJM cells contain a subpopulation producing IgL without IgH. In the plots in the lower row, cells at 24 hours after si[*IGLC*] treatment showed a leftward shift when compared with si[-] controls (top). This shift represents a marked decrease in IgL MFI. MFI values for IgL and IgH are shown for each plot, demonstrating that MFI for IgL decreases and for IgH increases with IgL knockdown. (B) In these flow cytometry histograms, the IgL and IgH in ALMC1 cells are shown at 24 hours after treatment with si[*IGLC*] or si[*IGH*]. The MFI is markedly reduced (arrows) in both instances consistent with a marked reduction in intracellular protein. (C) ALMC1 and EJM cells produce intact IgGλ and IgL. Specific interference with *IgL* or *IgH* mRNA leaves residual intracellular IgL or IgH staining as a percent of si[-] control. Plots reflect 3 independent repeats (median, range). Intracellular IgL MFI was reduced by a median of 72% in ALMC1 and 40% in EJM cells. (D) Reduction of IgL but not IgH or combined IgL and IgH production was associated with significantly reduced cell proliferation and viability by MTT assay at 24 hours (mean ± standard deviation [SD]). **P* < .01 by 2-tailed paired Student *t* test in both cases (ALMC1, n = 14; EJM, n = 9). (E) In ALMC1, ALMC2 (a sister cell line), and EJM cells, reduction of IgL but not IgH or IgL and IgH production was associated with significantly increased levels of caspase 3/7 activity at 24 hours (mean ± SD). **P* < .01 by 2-tailed paired Student *t* test; n = 4 for each cell line. (F) In ALMC1 cells producing intact IgGλ, specific interference with IgL mRNA is associated with increased intracellular IgH staining as this histogram demonstrates. In this typical example, MFI for IgH is increased by 41%.

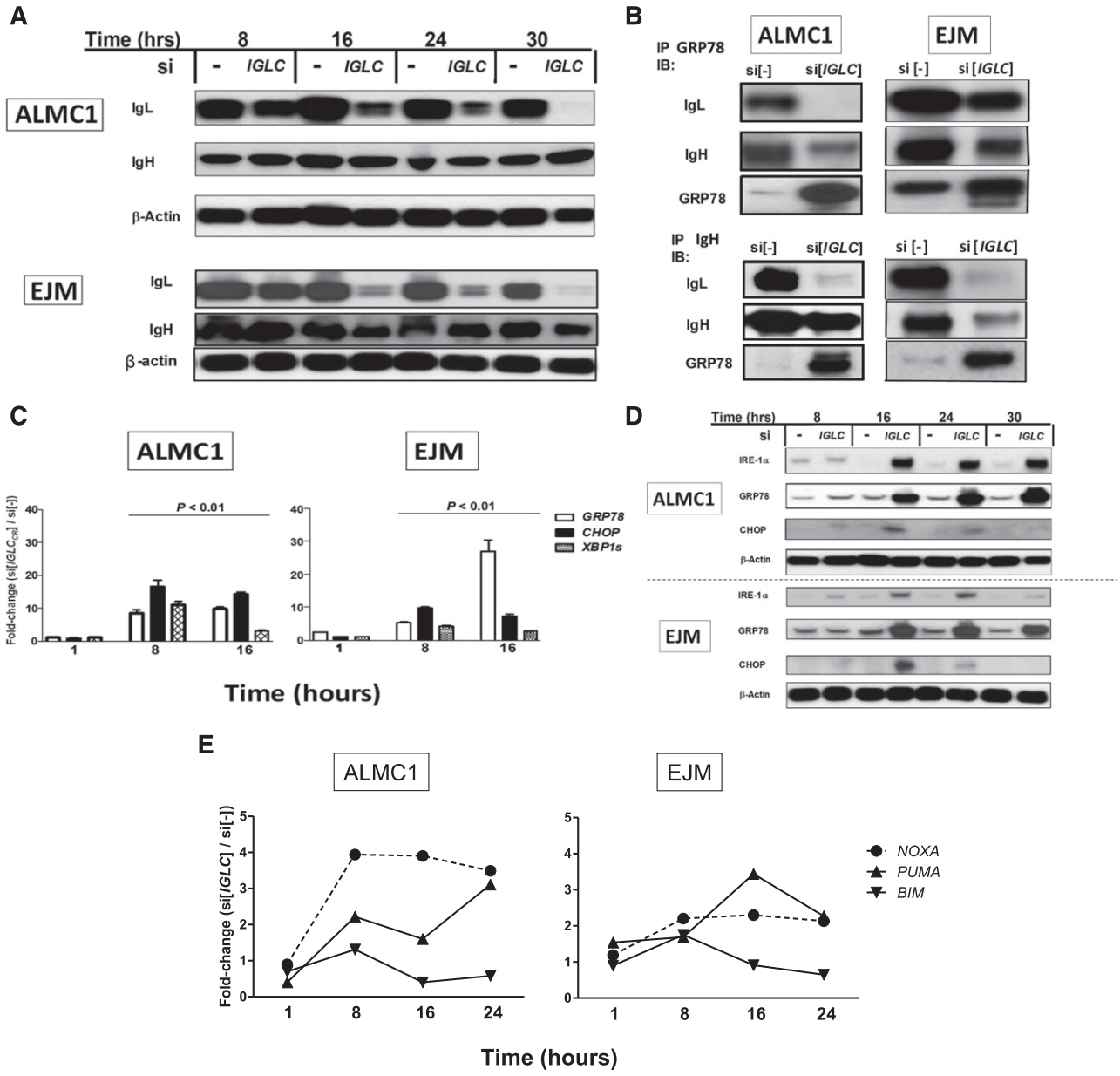

Figure 2. Intracellular unpaired IgH triggers the UPR and can cause apoptosis. (A) IBs from ALMC1 cells (top) treated with si[*IGLC*] or si[-] control over a 30-hour period show reduction in IgL and persistence of IgH intracellular proteins as do IBs of EJM cells (bottom) treated in the same way. (B) IBs of GRP78 and IgH IPs from ALMC1 and EJM cells treated with si[*IGLC*] or si[-] control show the coimmunoprecipitation of IgH with GRP78, as well as the marked decrease in IgL and increase in GRP78 that occur at 30 hours after si[*IGLC*] treatment. (C) Real-time PCR (qPCR) for markers of the UPR was performed with cDNA from ALMC1 and EJM cells treated with si[*IGLC*] or si[-] control for the indicated times. In si[*IGLC*]-treated cells, there were significant increases in all 3 UPR markers at 8 and 16 hours. Mean ± SD is shown with $P < .01$ compared with control by 2-tailed paired Student *t* test (n = 3). Three independent repeat qPCRs were performed in duplicate wells. (D) IBs for 3 markers of the UPR were performed with whole cell lysates from cells treated with si[*IGLC*] or si[-] control for the indicated times. As this typical IB shows, in si[*IGLC*]-treated but not control cells there were significant increases in all 3 UPR markers. (E) Real-time PCR (qPCR) for proapoptotic *BH3* family members was performed with cDNA from cells treated with si[*IGLC*] or si[-] control for the indicated times. In si[*IGLC*]-treated ALMC1 cells, there was a three- to-fourfold increase in *NOXA* expression maintained at 8, 16, and 24 hours. The increase in *NOXA* expression in EJM cells, however, was lower than in ALMC1 cells and also lower than the increase in *PUMA* expression. Two independent repeat qPCRs were performed in duplicate. (F) ALMC1 but not EJM cells treated with si[*IGLC*] displayed significantly increased levels of mitochondrial depolarization at 24 hours as represented by a significant decrease in the percentage of si[*IGLC*] relative fluorescence units (RFUs) of green JC-1 monomer compared with si[-] by flow cytometry. Increased levels of mitochondrial depolarization were not present when si[*IGLC*]-treated cells were cultured with 50 μM Z-VAD-FMK. Mean ± SD is shown with $*P = .01$ by 2-tailed paired Student *t* test (n = 3). (G) ALMC1 cells treated with si[*IGLC*] displayed increased levels of apoptosis manifest as annexin-V positivity at 24 hours. Viable cells were reduced to 64% with si[*IGLC*] treatment. Apoptosis did not occur when cells treated with si[*IGLC*] were cultured with a pan-caspase inhibitor (Z-VAD-FMK, 50 μM). (H) IB comparison of ALMC1 and EJM cells undergoing IgL knockdown shows that CHOP is markedly increased in ALMC1 compared with EJM cells. This IB is representative of 3 performed. (I) IP of myeloid cell leukemia sequence 1 (MCL-1) in ALMC1 and EJM cells treated with si[*IGLC*] indicates by IB that more NOXA is pulled down with MCL-1 from ALMC1 than from EJM cells. Normalized levels of MCL-1 and NOXA in si[*IGLC*] lanes are shown as percentages of si[-] levels. This IP/IB is a representative of 2 performed.

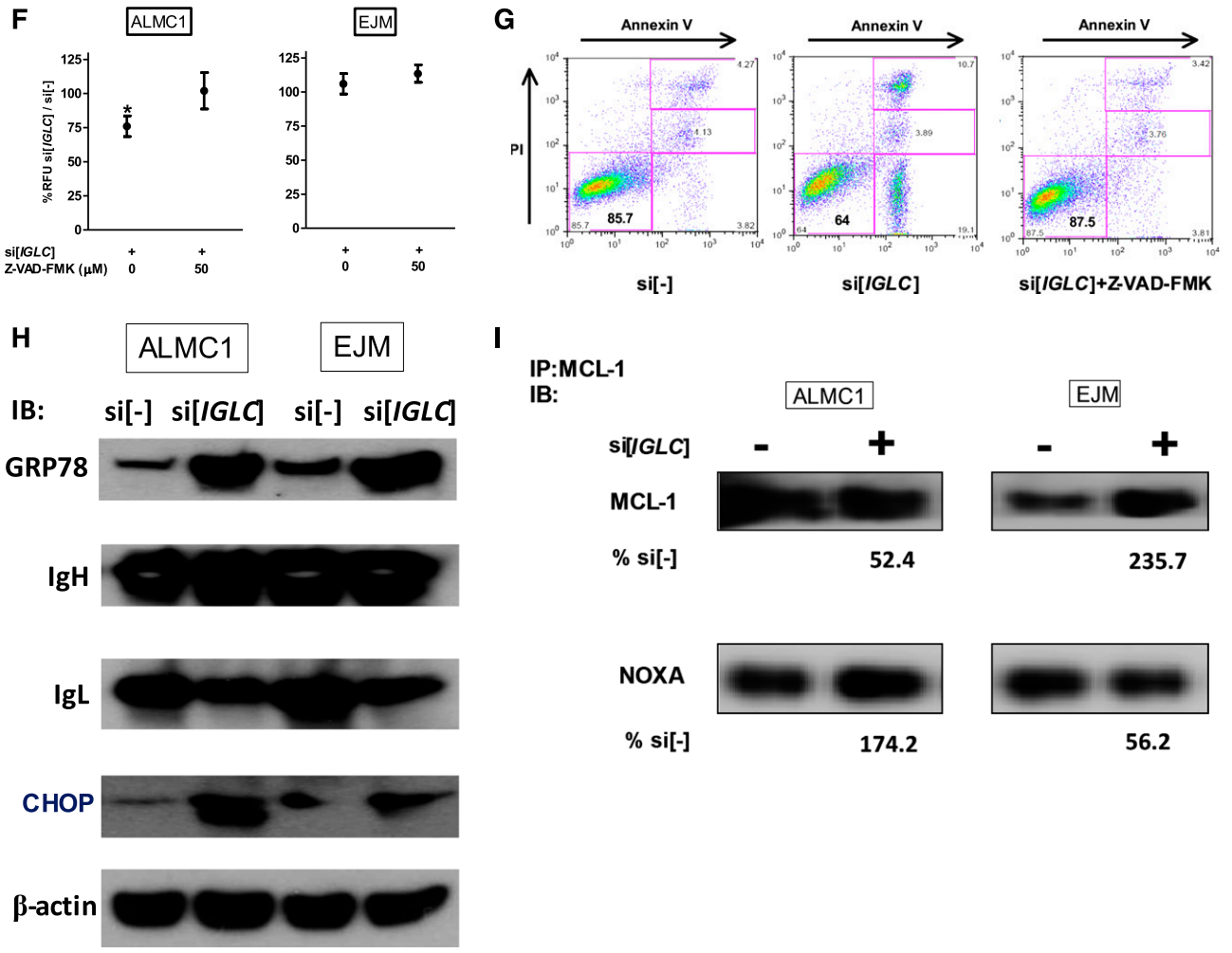

Figure 2. (Continued).

siRNA

Individual cell lines were evaluated for tolerance to streptolysin-O (Sigma-Aldrich) reversible permeabilization for transfection of siRNA, and the optimal effective concentrations of streptolysin-O and siRNA were determined. A similar approach testing tolerance was used for patient plasma cells (supplemental Figure 1; available on the *Blood* Web site).[13]

All siRNA agents were obtained from Dharmacon (Thermo Scientific, Lafayette, CO) using www.thermo.com/sidesign with modifications to minimize seed-region off-target effects (ON-TARGET*plus* SMART*pool*). The siRNA pools we used are in the supplemental Data, and custom-designed siRNA pools are defined in supplemental Table 1.

Caspase 3/7 assay

Luciferin-based caspase 3/7 activity assays (Promega, Madison, WI) were performed following the manufacturer's instructions on a Promega GloMax microplate luminometer in triplicate for each situation with 5×10^3 cells per well and reported as relative luminescence units.

MTT assay

The MTT [3-(4,5-dimethylthiazol-2-yl)-2,5-diphenyltetrazolium bromide] cell proliferation and viability assays (Invitrogen) were performed according to the manufacturer's instructions in triplicate with 2.5×10^4 cells per well and read on a microplate absorbance reader (BIO-RAD; Hercules, CA). Cell viability was also assessed by trypan blue staining where indicated.[14]

Flow cytometry

All antibodies used are listed in supplemental Table 2. Antibodies were titrated for optimal use and used with appropriate isotype controls. Flow cytometry was performed in our core facility on a FACSCalibur Cytometer (Becton Dickinson, Franklin Lakes, NJ). Mean fluorescence intensity (MFI) in each case was computed minus that of isotype control. Flow cytometry for intracellular immunoglobulin was performed with fluorescein isothiocyanate–conjugated anti-human IgG heavy chain and phycoerythrin-conjugated anti-human immunoglobulin λ-light-chain antibodies titrated for optimal use with appropriate isotype controls. Cells were permeabilized by using CytoFix/CytoPerm Fixation/Permeabilization kit (BD Pharmingen, Franklin Lakes, NJ), then stained with antibodies and acquired. MFI was analyzed with FlowJo (Tree Star, Ashland, OR).

The annexin-V/propidium iodide (PI) kit was from BD Pharmingen (San Jose, CA). As a control for annexin-V/PI staining, melphalan (L-phenylalanine mustard; Sigma-Aldrich) was dissolved in acid alcohol and used fresh at a concentration of 25 μM. For this assay, cells were harvested, washed twice, and suspended in annexin-V labeling buffer with fluorescein isothiocyanate–annexin V and PI as described in the kit and acquired. The percentage of apoptotic cells was computed with FlowJo.

Immunoblots (IBs) and immunoprecipitates (IPs)

All antibodies used are listed in supplemental Table 2. Cells were washed with phosphate-buffered saline, pelleted, and lysed in modified radioimmunoprecipitation assay buffer (Pierce/Thermo Scientific, Rockford, IL) with protease inhibitor cocktail (Roche Diagnostics, Indianapolis, IN) and

sodium pervanadate (Sigma-Aldrich) and MG132 (Millipore, Billerica, MA). After protein determination with bicinchoninic acid kit (Pierce/Thermo Scientific), equal amounts of denatured protein were subjected to 4% to 20% gradient sodium dodecyl sulfate–polyacrylamide gel electrophoresis and electroblotted onto Immobilon-P polyvinylidene difluoride transfer membrane (Millipore). After blocking nonspecific binding, blots were probed with appropriate primary antibodies and corresponding horseradish peroxidase–conjugated anti-rabbit or anti-mouse secondary antibodies. Signal was revealed with SuperSignal West Pico chemiluminescence reagent (Pierce/Thermo Scientific), detected by using ImageQuant LAS4000 mini and analyzed with ImageQuant TL (GE Healthcare Life Sciences, Pittsburgh, PA).

For immunoprecipitation, 200 μg of total lysate protein was precleared, antigen-specific antibodies were added, and the mix was incubated overnight at 4°C with rotation. Then 20 μL of protein A/G agarose beads was added, and the mix was further incubated for another 4 hours. After spinning down the beads and washing 3 times with modified radioimmunoprecipitation assay buffer/IP buffer, 25 μL of reducing sampling buffer was added to the pellets, and the suspension was reduced and denatured through boiling, ice chilling, and spinning at 15 000*g* for 10 minutes at room temperature. Equal volumes of cleared supernatants were subject to gradient sodium dodecyl sulfate–polyacrylamide gel electrophoresis, further blotting, and probing with antibodies.

Reverse-transcription qPCR

RNA was extracted and complementary DNA (cDNA) generated using standard methods.[15] Reverse-transcription quantitative polymerase chain reaction (qPCR) was performed in our core facility using TaqMAN Gene Expression Assays with all primers and probes from Applied Biosystems (Foster City, CA) on an Mx 3000P platform and related software (Stratagene, La Jolla, CA). For qPCR, expression levels were calculated using the $2^{-\Delta\Delta Ct}$ method. Primers and probes are listed in the supplemental Data.

Enzyme-linked immunosorbent assays (ELISA)

All antibodies used are listed in supplemental Table 2. Cultures were inoculated at a cell density of 10^6/mL of complete medium in all experiments for comparison and incubated for 1 day, and then supernatants of the suspensions were obtained from 3 independent repeat experiments for ELISA. For cells producing IgH and IgL, the same supernatants were used for measurements of both proteins. To measure the amounts of immunoglobulins in supernatants, quantitative ELISA was done by using anti-human IgG heavy chain and anti-human immunoglobulin λ-light-chain antibodies with sandwich enzyme-linked immunosorbent assays (Bethyl Laboratories, Montgomery, TX) according to the manufacturer's protocols. Optical density was read on a microplate reader (BIO-RAD), and protein quantity was calculated according to standard curves.

Microarray

Gene expression studies were performed using cDNA from 3 paired specimens of ALMC1 cells treated with si[$IGLC_{CR}$] or si[-] on the Illumina platform using the standard protocols for HumanHT-12 v4 Expression BeadChip at the Yale Center for Genome Analysis (New Haven, CT). The BeadStudio suite of programs was used to calculate the expression values for probe sets (Illumina Inc., San Diego, CA). These studies can be accessioned with National Center for Biotechnology Information Gene Expression Omnibus number GSE54507.

Statistics

PRISM (GraphPad, San Diego, CA) was used for descriptive statistics and analyses. All experiments were repeated a minimum of 3 times in triplicate wells unless otherwise noted. For microarray, Bioconductor packages Lumi/Limma were used to calculate the fold changes and *P* values.[16,17] TmeV was used to produce the heatmap of gene expression values for the regulated genes[18] whose expression differed by >1.5-fold with multiple hypothesis testing with $P < .10$. Web-based resource DAVID was used to calculate the enrichment of functional categories (DAVID Bioinformatics Resources 6.7, National Institute of Allergy and Infectious Diseases, National Institutes of Health).[19] The combined heatmap and Gene Ontology (GO) enrichment categories were generated using the GeneAnswers package in Bioconductor.[20]

Table 1. Potential target consensus sequences in λ-light-chain CR genes

IMGT* gene	Nucleotides†	Sequences
J00252	49-67	ctccaagccaacaaggcca
X51755	55-73	ctccaagccaacaaggcca
J00253	55-73	cttcaagccaacaaggcca
X06875	55-73	cttcaagccaacaaggcca
J00254	49-67	cttcaagccaacaaggcca
K01326	55-73	cttcaagccaacaaggcca
X06876	55-73	cttcaagccaacaaggcca
D87017	55-73	cttcaagccaacaaggcca
J03011	55-73	cttcaagccaacaaggcca
X51755	55-73	cttcaagccaacaaggcca
M61771	55-73	cttcaagccaacaaggcca
Target 1		CTTCAAGCCAACAAGGCCA
J00252	104-122	ctgtgacagtggcttggaa
X51755	110-128	ctgtgacagtggcctggaa
J00253	110-128	ccgtgacagtggcttggaa
X06875	110-128	ccgtgacagtggcctggaa
J00254	104-122	ccgtgacagttgcctggaa
K01326	110-128	cagtgacagttgcctggaa
X06876	110-128	ccgtgacagtggcctggaa
D87017	110-128	ccgtgacagtggcctggaa
J03011	110-128	ctgtgaaagtggcctggaa
X51755	110-128	ccgtgacagtggcctggaa
M61771	110-128	ccgtgacagtggcctggaa
Target 2		CCGTGACAGTGGCCTGGAA
J00252	161-182	ccaaacagagcaacaacaa
X51755	176-194	ccaaacagagcaacaacaa
J00253	176-194	ccaaacaaagcaacaacaa
X06875	176-194	ccaaacaaagcaacaacaa
J00254	170-188	ccaaacaaagcaacaacaa
K01326	176-194	ccaaacaaagcaacaacaa
X06876	176-194	ccaaacaaagcaacaacaa
D87017	176-194	ccaaacaaagcaacaacaa
J03011	176-194	ccaaacagagcaacaacaa
X51755	176-194	ccaaacaaagcaacaacaa
M61771	176-194	ccaaacaaagcaacaacaa
Target 3		CCAAACAAAGCAACAACAA
J00252	217-235	acgcccgagcagtggaagt
X51755	223-241	acgcccgagcagtggaagt
J00253	223-241	acgcctgagcagtggaagt
X06875	223-241	acgcctgagcagtggaagt
J00254	217-235	acgcctgagcagtggaagt
K01326	223-241	acgcctgagcagtggaagt
X06876	223-241	acgcctgagcagtggaagt
D87017	223-241	acgcctgagcagtggaagt
J03011	223-241	acgcctgagcagtggaagt
X51755	223-241	acgcccgagcagtggaagt
M61771	223-241	acgcccgagcagtggaagt
Target 4		ACGCCTGAGCAGTGGAAGT

*IMGT = ImMunoGeneTics information system, www.imgt.org.
†Numeration is sense strand 5′ to 3′.

Results

Knockdown of IgL not IgH causes effector caspase activation

With siRNA targeted to the IgL or IgH variable region mRNA of ALMC1 (and ALMC2) or EJM cells,[10,21] at 24 hours expression of IgL was reduced as appreciated by flow cytometry dot plot (Figure 1A), and expression of either IgL or IgH was reduced as shown by flow cytometry histograms (Figure 1B) and by differences in

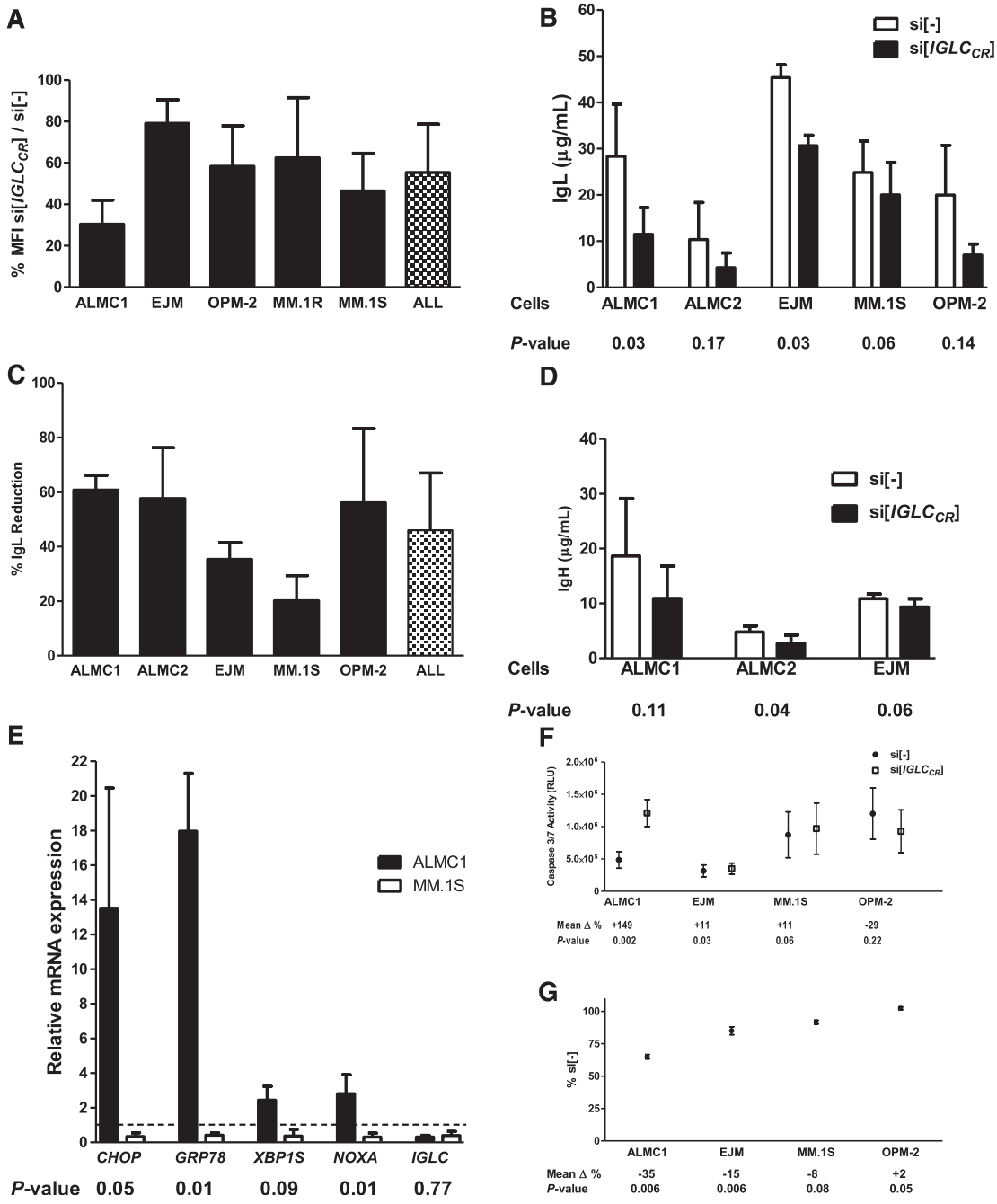

Figure 3. Knockdown of the IgL CR reduces immunoglobulin secretion and cell viability. (A) Five human MM cell lines that secrete IgL were treated with si[$IGLC_{CR}$] targeting the CR of the *IgL* mRNA or si[-] control, and the residual MFI at 20 hours after knockdown is shown. Mean ± SD; n = 3 observations per cell line. In all (n = 15), the mean MFI of intracellular IgL after si[$IGLC_{CR}$] treatment was 55% ± 23% of control indicating a 45% average reduction in less than a day. (B) The concentrations of secreted IgL in culture supernatants from these 5 human MM cell lines after treatment with si[$IGLC_{CR}$] or si[-] control were measured by ELISA. Cultures were charged with 10^6 cells per mL, and supernatant was obtained 24 hours later for measurement. All cells treated with si[$IGLC_{CR}$] secreted less IgL. Mean ± SD is shown for 3 independent repeats per cell line with *P* values obtained with 2-tailed paired Student *t* test. (C) This graph shows the percent reductions in secreted IgL with si[$IGLC_{CR}$] treatment. Mean ± SD is shown for 3 independent repeats per cell line. The mean percent reduction for all 15 observations was 45% ± 23%. (D) The concentrations of secreted IgH in culture supernatants from 3 human MM cell lines that secrete intact IgGλ after treatment with si[$IGLC_{CR}$] or si[-] control were measured by ELISA. Mean ± SD is shown for 3 independent repeats per cell line with *P* values obtained with 2-tailed paired Student *t* test. The mean reductions in secreted IgH were 45% ± 9%, 43% ± 22%, and 14% ± 8% for ALMC1, ALMC2, and EJM cells, respectively. (E) ALMC1 as IgGλ-producing cells were compared with MM.1S as IgL-only producing cells for evidence of activation of the UPR and change in the expression of *NOXA* by qPCR. At 20 hours after treatment, the relative fold changes in expression of the UPR markers *GRP78*, *CHOP*, and *XBP1S*, and of *NOXA*, with si[$IGLC_{CR}$] are substantial in cells producing IgGλ but not IgL only. Assays were performed 3 times with cDNA from 3 independent repeat experiments. Mean ± SD is shown with *P* values obtained with 2-tailed unpaired Student *t* test. Dotted line is qPCR control. (F) Caspase 3/7 activity was measured with the GloMax bioluminescence assay in 2 myeloma cell lines that produce intact IgGλ (ALMC1 and EJM) and 2 that produce only IgL (MM.1S and OPM-2) after treatment with si[$IGLC_{CR}$] or si[-]. Reductions in IgL in cells producing intact IgGλ were associated with significantly increased caspase 3/7 activity, whereas in cells producing only IgL there was no increase in caspase 3/7 activity associated with IgL reductions. (In OPM-2 cells, there was an apparent decrease in caspase 3/7 activity with IgL knockdown.) Mean ± SD of the changes in caspase 3/7 activity and *P* values are shown, the latter obtained with 2-tailed paired Student *t* test (n = 3 for each cell line). (G) Cell viability and proliferation were measured by MTT assay in 2 myeloma cell lines that produce intact IgGλ (ALMC1 and EJM) and in 2 that produce only IgL (MM.1S and OPM-2) after treatment with si[$IGLC_{CR}$] or si[-]. Reductions in IgL in cells producing intact IgGλ were associated with significantly decreased cell viability and proliferation, whereas in cells producing only IgL there was no decrease compared with si[-] controls. Mean ± SD of the changes in MTT readouts and *P* values are shown, the latter obtained with 2-tailed paired Student *t* test (n = 3 for each cell line).

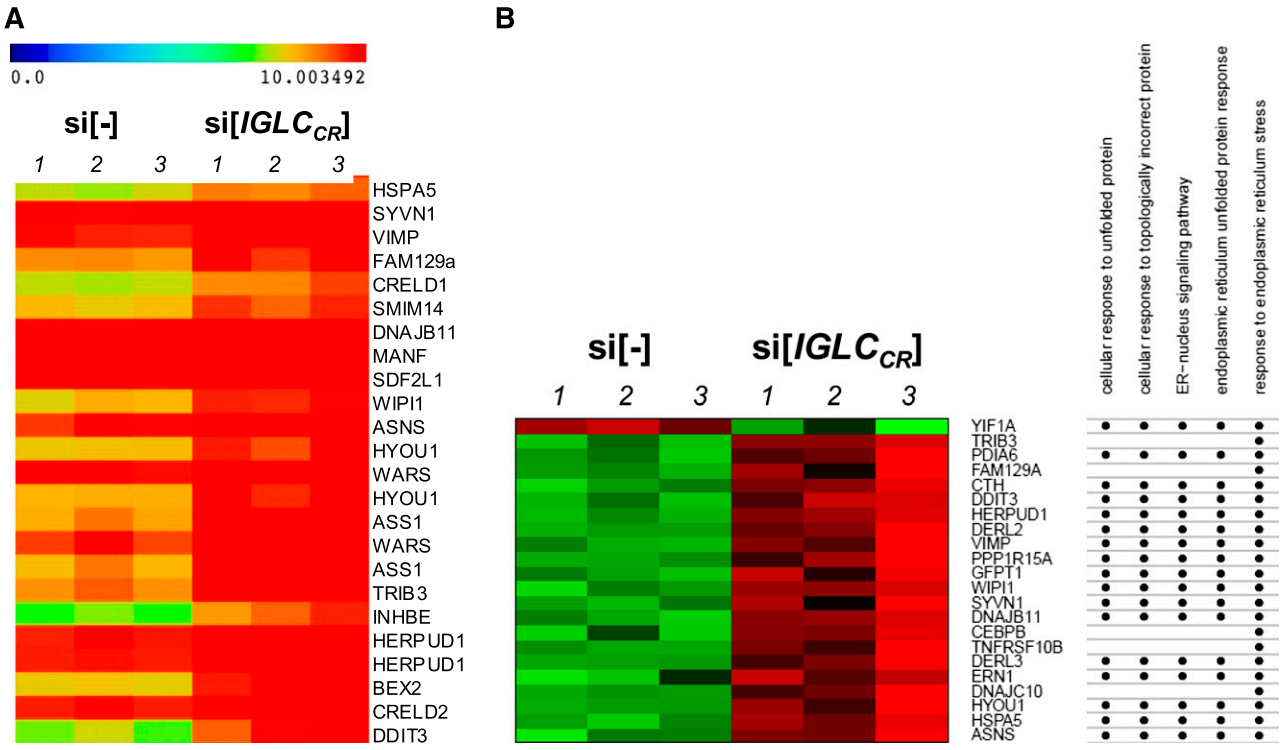

Figure 4. Treatment with si[*IGLC$_{CR}$*] triggers ER stress and NOXA-related apoptosis. (A) Gene expression studies were performed using cDNA from 3 paired specimens of ALMC1 cells treated with si[*IGLC$_{CR}$*] or si[-] on the Illumina platform using the standard protocols for HumanHT-12 v4. Expression BeadChip and the BeadStudio suite of programs were used to calculate the expression values for probe sets (Illumina Inc.). A heatmap of the 99 genes whose expression differed >1.5-fold between si[-] control and si[*IGLC$_{CR}$*]-treated samples by multiple hypothesis testing at $P < .10$ is shown in supplemental Figure 3, increasing in expression from top to bottom. *PMAIP1* (*NOXA*) is indicated in the supplemental figure with 1.54-fold increased expression in cells treated with si[*IGLC$_{CR}$*]. The 24 genes that were most upregulated in cells treated with si[*IGLC$_{CR}$*] are shown in this figure. *HSPA5* (*GRP78*) is upregulated 2.4-fold. *CHOP* (also known as *DDIT3*) is the most upregulated gene consistent with activation of a terminal ER stress response. (B) GO heatmap was generated with GeneAnswers package in Bioconductor and shows gene expression values and pathways involved for the regulated genes, indicating that the UPR, ERAD, and apoptotic pathways are notably involved.[18] (C) In this IB of si[-] control and si[*CHOP*]-, si[*IGLC$_{CR}$*]-, and si[*IGLC$_{CR}$*+*CHOP*]-treated ALMC1 cells, there were reductions in CHOP in the si[*CHOP*] and double knockdown cells; whereas in the si[*IGLC$_{CR}$*] and double knockdown cells there were increases in GRP78, IRE1α, NOXA, MCL-1, and cleaved poly ADP ribose polymerase. (D) In ALMC1 cells at 20 hours after treatment, reduction of *IgL* expression was associated with increased caspase 3/7 activity, whereas simultaneous reduction of *IgL* and *NOXA* was associated with substantially reduced caspase 3/7 activity. Cells in which *NOXA* alone was knocked down had on average 17% less caspase 3/7 activity than controls. Mean ± SD with *P* value obtained with 2-tailed unpaired Student *t* test (n = 9). (E) In this IB of si[-] control and si[*NOXA*]-, si[*IGLC$_{CR}$*]-, and si[*IGLC$_{CR}$* + *NOXA*]-treated ALMC1 cells, there were increases in GRP78, IRE1α, and phosphorylated PERK in si[*IGLC$_{CR}$*]-treated cells; reductions in NOXA in the si[*NOXA*] and double knockdown cells; but no differences in the levels of MCL-1 with *NOXA* knockdown.

MFI (Figure 1C). With this approach to knockdown of IgL, IgH, or IgL and IgH, reductions in cell viability and proliferation and increases in caspase 3/7 activity were observed in cells with IgL but not IgH or IgL and IgH knockdown (Figure 1D-E). With IgL knockdown, increased intracellular staining for IgH was observed (Figure 1A,F).

Knockdown of IgL activates the UPR and causes an ER stress response

After knockdown of IgL in clonal cells making IgGλ, IgH production was maintained, whereas intracellular IgL was diminished (Figure 2A). From lysates of control si[-] and si[*IGLC*]-treated cells, IgH was pulled down to assess IPs for IgL and for the chaperone glucose-regulated protein 78 kDa (GRP78). The results (Figure 2B) show that IgH is associated with GRP78. Moreover, IP of GRP78 shows association with IgH as well, although we note that in the IBs from both cell lines there may be contamination in the IgH lanes by the IP antibody for GRP78. Nevertheless, the relevant features of IgL knockdown, GRP78 induction, and IgH/GRP78 association can be appreciated.

The UPR is triggered by dissociation of GRP78 from the activators inositol-requiring enzyme 1 alpha (IRE1α), protein kinase RNA–like ER kinase (PERK), and activating transcription factor 6.[22] In Figure 2C, prompt activation of the UPR is seen with expression of *CHOP*,[23] *GRP78*, and *XBP1s*. In Figure 2D, increased production of IRE1α, GRP78, and C/EBP homologous protein (CHOP) is seen within hours of UPR activation. Given the evidence for likely caspase-dependent apoptosis with IgL knockdown, the timeline of changes in expression of proapoptotic Bcl-2 homology 3 domain only family members was studied, and fourfold upregulated expression of *NOXA* and upregulated expression of *PUMA* but not *BIM* in ALMC1 cells, and to a lesser degree of *PUMA* and *NOXA* in EJM cells, was seen (Figure 2E). Moreover, by 20 hours after IgL knockdown, 25% of ALMC1 cells showed evidence of mitochondrial depolarization reversible by pan-caspase inhibition, consistent with the results in Figure 1D-E, and therefore caspase dependent (Figure 2F). EJM cells treated in the same way did not display increased levels of mitochondrial depolarization. By annexin-V/PI staining, in ALMC1 cells there was an average of 29.8 ± 6.8% specific apoptosis associated with IgL knockdown (n = 3) and none with IgH or combined IgL and IgH knockdown. Pan-caspase inhibition reversed this effect (Figure 2G). In EJM cells, despite the modest increase in caspase 3/7 activity appreciated by bioluminescence (Figure 1E) and the transient upregulation of *NOXA* (Figure 2E), evidence of mitochondrial depolarization by 5,5′,6,6′-tetrachloro-1,1′,3,3′-tetraethylbenzimi-dazolylcarbocyanine iodide (JC-1) staining (Figure 2F) and of early or late apoptosis by annexin-V/PI staining was not found (data not shown).

The differences between ALMC1 and EJM cells were then examined further. ALMC1 cells produce an intact IgGλ with excess IgL,

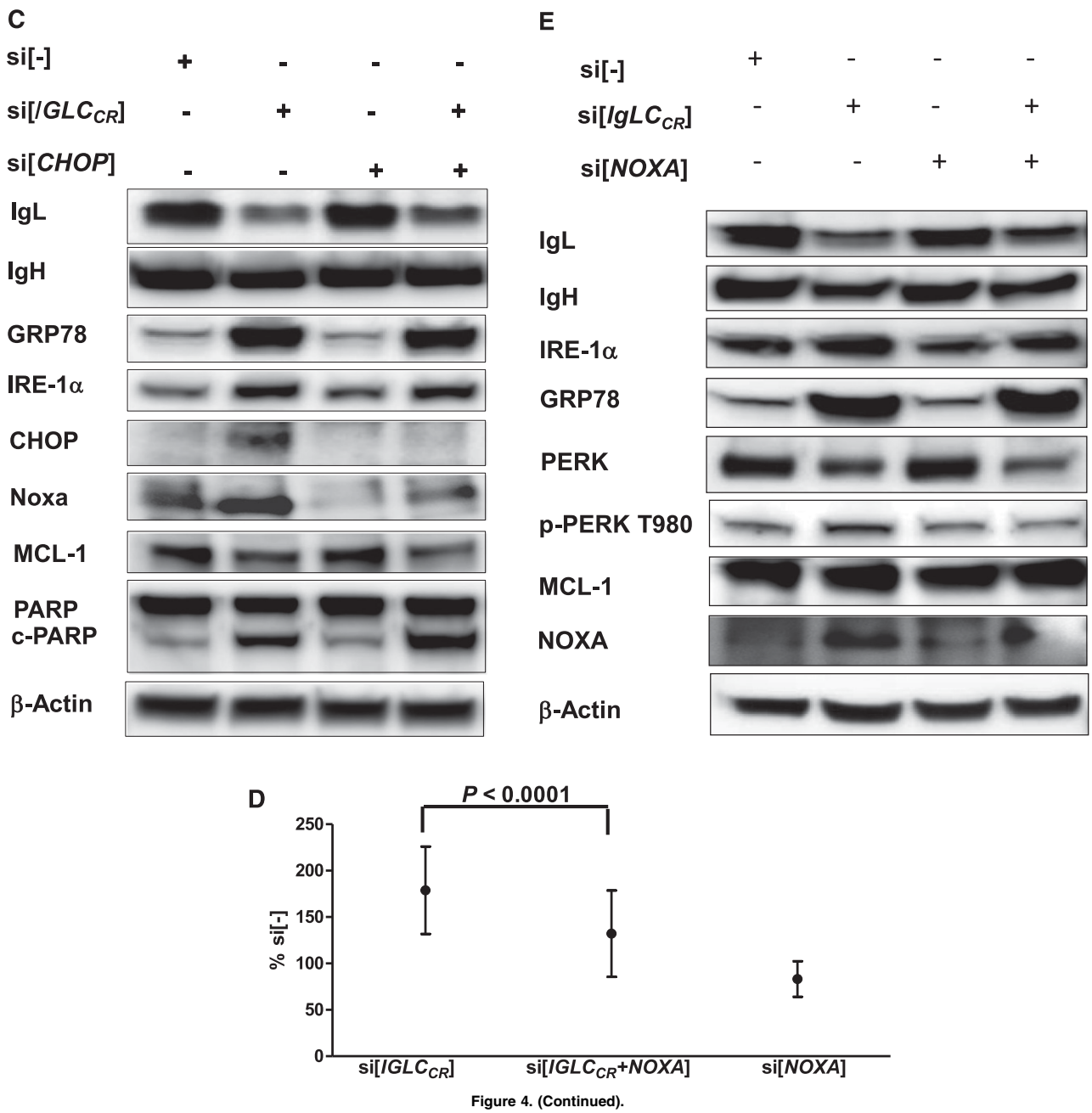

Figure 4. (Continued).

whereas EJM cells have 2 populations by flow cytometry, including a minor one that makes IgL only (Figure 1A). The efficiency of IgL knockdown with variable region siRNA was lower in EJM than in ALMC1 cells (Figure 1C), and the relative decrease in cell viability and proliferation (Figure 1D) and increase in caspase 3/7 activity with IgL knockdown were also smaller in EJM than ALMC1 cells (Figure 1E). (Of note, the efficiency of *GAPDH* knockdown was best in ALMC1 cells; supplemental Figure 1). Both cell lines, however, have similar timelines of IgL knockdown (Figure 2A), and both show the coassociation of IgH and GRP78 (Figure 2B) and activation of the UPR (Figure 2C-D). Unlike the *CHOP* preeminent pattern of UPR activation in ALMC1 cells, a *GRP78* preeminent pattern occurs in EJM cells (Figure 2C).

In ALMC1 cells, CHOP is significantly increased compared with EJM cells (Figure 2H), and there was more NOXA, an MCL-1 antagonist, pulled down with MCL-1 from ALMC1 than from EJM cells (Figure 2I). CHOP is viewed as a mediator of a terminal UPR, and MCL-1, an antiapoptotic Bcl-2 family member, as a critical comediator of apoptosis in human myeloma cells.[24,25] These results are consistent with a terminal ER stress response in ALMC1 but not EJM cells.

Multiple factors may contribute to this difference, including the presence of an IgL-only subpopulation of EJM cells and the lower efficiency of IgL knockdown in EJM cells, as well as the differences between ALMC1 and EJM cells with respect to the ratios of IgL and IgH production (shown subsequently) and the production by EJM cells of IgL of 2 different sizes (supplemental Figure 2). Although the process of intact antibody formation is disrupted by IgL knockdown, the amount of IgL available in EJM cells may be adequate to match the amount of intracellular IgH waiting to be paired.

Treatment of plasma cells with si[$IGLC_{CR}$] reduces immunoglobulin secretion and cell viability

In order to design si[$IGLC_{CR}$], 1 pool of siRNA specific for *IgL* CR, 4 consensus region targets in the *IgL* CR were identified. Each target is listed below the relevant CR consensus sequence in Table 1 (the pool is in supplemental Table 1). The availability of 1 pool would in theory allow reduction of IgL production and secretion in multiple specimens without regard for variable region sequences; it would also allow an evaluation of the differences in secretion between ALMC1 and EJM cells using the same reagent. (Subsequently, the *IgL* CR of both cell lines was determined to be concordant with the siRNA targets; data not shown.)

Five human myeloma cell lines that produce IgL were treated with si[$IGLC_{CR}$], demonstrating a 45% average reduction in intracellular IgL MFI after less than a day (Figure 3A) and by ELISA an overall reduction of IgL secretion of 45% (Figure 3B-C). IgH secretion was markedly reduced as well at 1 day after IgL knockdown (Figure 3D). EJM cells secreted the most IgL (Figure 3B). When treated with si[$IGLC_{CR}$], EJM cells secreted ~35% less IgL in 1 day than control cells (Figure 3C). In comparison, ALMC1 cells treated with si[$IGLC_{CR}$] secreted ~60% less (Figure 3B-C). EJM cells also secreted about half the amount of IgH produced by ALMC1 cells, and when treated with si[$IGLC_{CR}$] secreted only 14% less IgH; in contrast, ALMC1 cells treated with si[$IGLC_{CR}$] secreted almost 50% less IgH (Figure 4D). This difference led to the concept that the ratio of postknockdown IgL and basal IgH secretion might be related to the triggering of the terminal UPR. This ratio was greater in EJM cells at 3 (30 μg/mL ÷ 10 μg/mL per day per million cells) vs 0.5 (10 μg/mL ÷ 20 μg/mL) in ALMC1 cells. There likely were lower levels of unpaired IgH in EJM than in ALMC1 cells with IgL knockdown, a difference that may contribute to the lack of a terminal ER stress response in EJM cells.

To examine further the activation of the UPR and changes in *NOXA* expression with CR knockdown, ALMC1 cells that secrete both intact IgGλ and IgL were compared with MM.1S cells that secrete only IgL. As shown in Figure 3E, *CHOP*, *GRP78*, *XBP1S*, and *NOXA* were all substantially upregulated in ALMC1 but not in MM.1S cells, whereas the efficiency of IgL knockdown was the same for both. Caspase 3/7 activity and cell viability and proliferation were then studied after si[$IGLC_{CR}$] treatment, and the former was increased and the latter decreased significantly in cells making intact IgGλ (Figure 3F-G).

The terminal ER stress response with si[$IGLC_{CR}$] treatment is NOXA dependent

The heatmap of genes significantly regulated in ALMC1 cells by si [$IGLC_{CR}$] treatment is shown in supplemental Figure 3. *CHOP* (also known as *DDIT3*) is the most highly upregulated gene. The detailed depiction of the most upregulated genes (Figure 4A) and the integrated view provided by a GO heatmap (Figure 4B) of the functional classes of activated genes demonstrate that a high level of ER stress is induced by the load of unpaired IgH and that genes involved in the UPR and endoplasmic-reticulum–associated protein degradation (ERAD) are upregulated in concert.

The circuitry of intrinsic terminal ER stress responses in clonal plasma cells remains unclear. The IRE1α pathway and the downstream activation of c-Jun N-terminal kinase by phosphorylated apoptosis signal-regulating kinase 1 (ASK1)[26] can lead to apoptosis of plasma cells. Arachadonic acid can inhibit ASK1 phosphorylation in plasma cells by activating protein phosphatase 5. In cells treated with si[$IGLC_{CR}$], however, there was no increase in phosphorylated c-Jun N-terminal kinase at 24 hours by IB and no effect of arachadonic acid at 72 hours by MTT assay, suggesting that IRE1α-mediated activation of ASK1 did not play a significant role in si[$IGLC_{CR}$]-related apoptosis (data not shown).

A simultaneous double knockdown technique was then employed, asking whether simultaneous knockdown of IgL expression along with *CHOP* or *NOXA* would change the level of caspase 3/7 activity. There was no difference in the levels of caspase 3/7 activity between si[$IGLC_{CR}$]- and si[$IGLC_{CR}$+*CHOP*]-treated cells at 169 ± 31% and 170 ± 34% of controls, respectively ($P = .87$, n = 5), whereas si[*CHOP*]-treated cells had levels that were 102 ± 43% of controls. Also, cells treated with si[$IGLC_{CR}$+*CHOP*] showed increased levels of NOXA as did si[$IGLC_{CR}$]-treated cells (Figure 4C). In contrast, si[$IGLC_{CR}$+*NOXA*] treatment significantly reduced caspase 3/7 activity (Figure 4D-E). Although *NOXA* upregulation had been noted in EJM cells (Figure 2E), increased expression began earlier, was greater, and was observed for a longer time in ALMC1 than in EJM cells (Figure 2E), consistent with the comparative increase of NOXA in ALMC1 cells in the IP of MCL-1 (Figure 2I).

Treatment of patient plasma cells with si[$IGLC_{CR}$] reduces IgL production and increases caspase 3/7 activity

With CD138-selected specimens from patients with AL, highly enriched suspensions of plasma cells were secured.[11] The patient characteristics, number, and uses of specimens are detailed in supplemental Table 3. In Figure 5A, an example of prompt and effective treatment with si[$IGLC_{CR}$] causing an 85% reduction in intracellular IgL immunofluorescence is shown. In supplemental Figure 4, IBs of 2 specimens are shown, demonstrating significant reductions in IgL with si[$IGLC_{CR}$] treatment. As shown in Figure 5B, in 16 specimens evaluated by qPCR, the average reduction in *IgL* message exceeded 70%, and as shown in Figure 5C, in 13 specimens evaluated by flow cytometry the average reduction in MFI was 51%. In 10 instances for which there are both qPCR and flow cytometry data, as shown in Figure 5D, the reductions in MFI were significantly correlated with the reductions in message by linear regression analysis ($r^2 = 0.56$, $P < .01$). In 5 instances, the plasma cells made both an intact immunoglobulin and IgL, and in those cases, a pattern of increased intracellular IgH immunofluorescence related to the degree of reduction of IgL immunofluorescence could be seen (Figure 5E).

Caspase3/7 activity was evaluated with si[$IGLC_{CR}$] or si[-] in 6 specimens making IgL only, giving relative luminescence units of 24 186 ± 19 114 and 22 999 ± 15 772 in si[$IGLC_{CR}$]-treated and si[-] control aliquots, respectively ($P = .57$, 2-tailed paired Student *t* test). In contrast, when caspase 3/7 activity was evaluated in 5 specimens making intact antibodies, as shown in Figure 5F, there was a significant increase in caspase 3/7 activity with si[$IGLC_{CR}$] treatment ($P = .04$, 2-tailed paired Student *t* test). These results support the conclusion that 1 siRNA pool targeting consensus sequences in the *IgL* CR message can effectively reduce both *IgL* message and IgL protein production without regard for the diversity of *IgL* variable region sequences and can also trigger a terminal ER stress response in cells making intact antibodies.

Discussion

We report that the targeting of consensus sequences in the CR of λ-light-chain genes with 1 pool of siRNA (si[$IGLC_{CR}$]) can

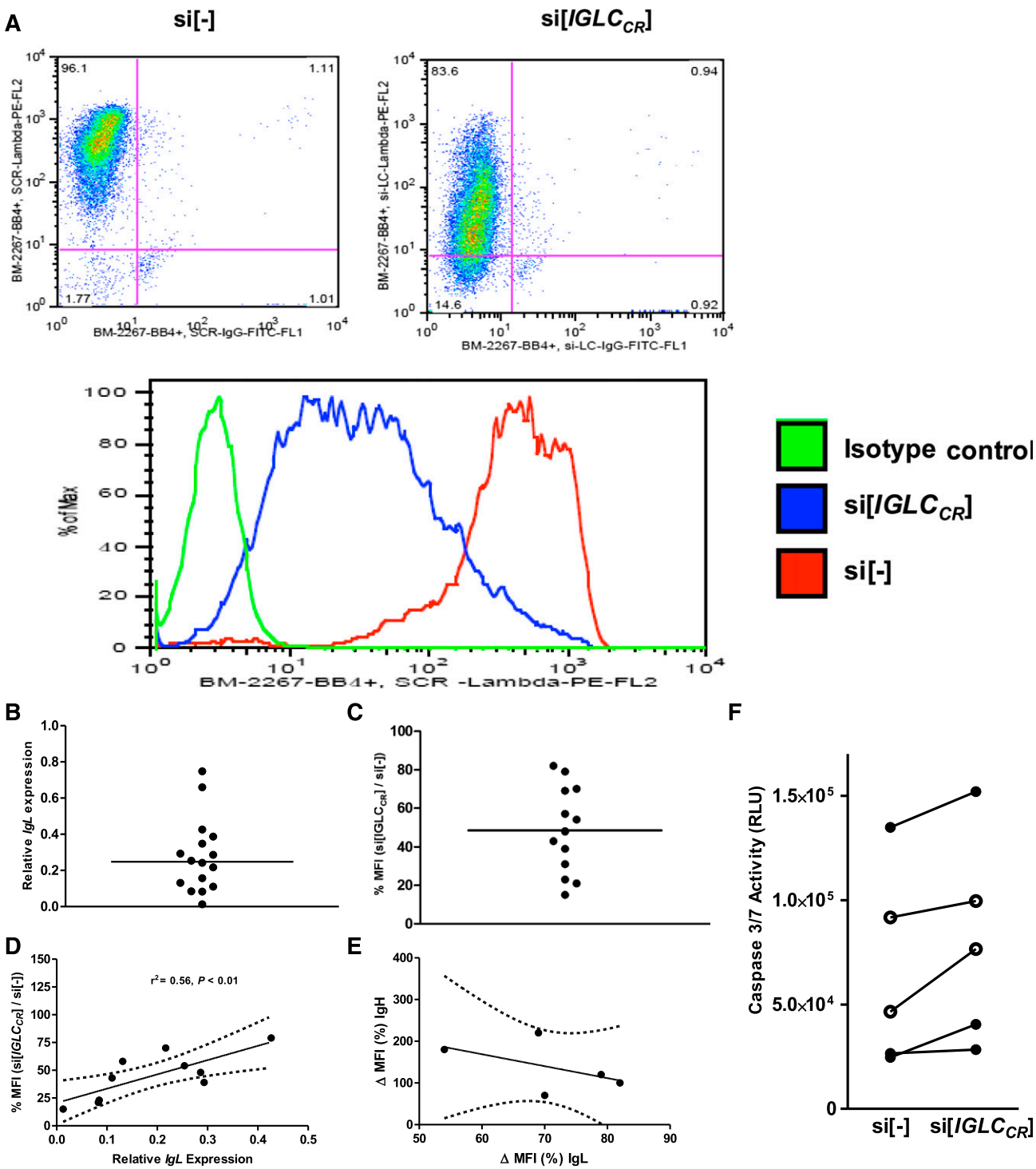

Figure 5. Treatment with si[*IGLC*$_{CR}$] in patient cells reduces IgL. (A) A flow cytometry plot of CD138$^+$ marrow plasma cells from a patient with a λ-light-chain monoclonal gammopathy causing systemic AL shows the results of treatment with si[*IGL*$_{CR}$] or si[-]. The upper panel shows the marked reduction in IgL at 20 hours, and the lower panel shows histograms indicating a reduction of MFI in si[*IGLC*$_{CR}$]-treated cells of 85%. (B) Real-time PCR (qPCR) was performed on CD138$^+$ plasma cells (from patients with AL) treated with si[*IGLC*$_{CR}$] or si[-] control. Overall the average residual λ-light-chain message by qPCR was 0.28 ± 0.2 of control (mean ± SD; mean is shown in figure, n = 16). (C) Flow cytometry for intracellular IgL was performed on CD138$^+$ plasma cells (from patients with AL) treated with si[*IGLC*$_{CR}$] or si[-] control, showing that the average residual MFI was 49% (n = 13). (D) In 10 cases, we had sufficient CD138$^+$ plasma cells to perform both qPCR (>4 × 10^5) and flow cytometry (>10^6) after treatment with si[*IGLC*$_{CR}$] or si[-] control. The correlation is shown between residual MFI and residual message by linear regression (line of best fit) with 95% confidence intervals (r^2 = 0.56, P < .01). (E) In 5 specimens, both the intracellular IgL and IgH in CD138$^+$ cells were evaluated simultaneously by flow cytometry after si[*IGLC*$_{CR}$] treatment. This figure suggests that the lower the IgL MFI became with si[*IGLC*$_{CR}$] treatment, the higher the residual intracellular IgH MFI became (P > .05). (F) Five specimens of CD138$^+$ plasma cells from patients with AL and abnormal λ-light-chain levels but with immunoglobulin heavy chains (IgGλ = 4, IgAλ = 1; open circles are 2 specimens from the same patient 3 months apart) were treated with si[*IGLC*$_{CR}$] or si[-]. Caspase 3/7 activity was evaluated by bioluminescence 20 hours later, and significantly higher levels of caspase 3/7 activity were seen with si[*IGLC*$_{CR}$] treatment. (P = .04 with 2-tailed paired Student t test).

rapidly and substantially reduce λ-light-chain (IgL) production in numerous clones of λ plasma cells without regard for the diversity of the variable regions. Moreover, in λ plasma cells making intact immunoglobulin, si[$IGLC_{CR}$] also can activate both UPR and ERAD with terminal potential because of the stress associated with unpaired IgH in the ER. Preliminary data indicate that the terminal potential is inversely related to the ratio of residual IgL to basal IgH, a hypothesis amenable to further testing. The ratio depicts the relative availability of a light chain to pair with a heavy: with a ratio of <1, both the excess of unpaired IgH and the ER stress-related terminal potential may be higher.

Activation of the UPR is a complex interplay of pathways that can be associated with either restored homeostasis or apoptosis.[27] The UPR is constitutively activated in plasma cells as they differentiate from B cells with increased demand for protein folding and ER trafficking capacity; it is particularly the activity of spliced form of X-box-binding protein 1 that escorts the metamorphosis of B cells into morphologically distinct antibody-producing cells.[6] In myeloma, the UPR has been a major theme in the study of the mechanisms of action of proteasome inhibitors.[28-31] The importance of the PERK–activating transcription factor 4–CHOP arm of the UPR as a potential indicator of caspase-dependent apoptosis highlights a paradoxical aspect of the role of the UPR in plasma cell biology.[32]

In this report, knockdown of IgL production and accumulation of unpaired intracellular IgH activate the UPR and ERAD in plasma cells making intact immunoglobulins but not in plasma cells making only IgL. Of note, the loss of IgH production with manufacture of only IgL and the possible toxicity of IgH to plasma cells are fundamental themes in plasma cell biology.[7,33-36] After passage in culture, hybridomas often lose IgH production and make IgL only, and the majority of human myeloma cell lines produce IgL without IgH partners.[33] IgL-deficient mice attain a complete block in B-cell development at the stage when light-chain rearrangement should occur, resulting in surface IgM deficiency, retention of unpaired IgH in the cytoplasm, and lack of plasma cells.[37] Normal human plasma cells make more IgL than IgH, possibly to minimize intracellular accumulation of unpaired IgH.[38] In 20% of cases of multiple myeloma, only IgL is made.[39] Moreover, when myeloma relapses after the plateau phase, we often observe "light-chain escape," the emergence of a modified phenotype in which IgL replaces, or is produced far in excess of, IgH.[40,41]

The model of terminal UPR and ERAD activation that we report is caspase and NOXA dependent. Regulation of *NOXA* has been related to DNA damage as well as ERAD and epigenetic changes that enhance the activity of specific transcription factors; moreover, in vitro, bortezomib-induced apoptosis has been shown to depend on NOXA.[42-45] The model we report provides the opportunity to investigate in greater detail how plasma cells may overcome, adapt, or succumb to intrinsic terminal ER stress signals.

siRNA therapeutics are in clinical trials for transthyretin-related amyloidosis, delivered via lipid nanoparticles targeting hepatic cells producing transthyretin[46]; moreover, investigators interested in AL have recently demonstrated that RNA interference with IgL production is feasible and merits further study.[47,48] Targeting specific types of cells, such as clonal marrow plasma cells, for RNA interference poses additional major challenges. The significance of the results with si[$IGLC_{CR}$] with respect to turning off IgL production and secretion may prove relevant to light-chain-mediated diseases. Some of the AL patient samples treated with si[$IGLC_{CR}$] were obtained from patients whose plasma cell disease had not responded to conventional therapies including bortezomib; the reduction of *IgL* message in si[$IGLC_{CR}$]-treated cells may reflect the importance of RNA degradation to the malignant plasma cell phenotype,[49] and, although the reductions were in some cases substantial, they were also notably variable, accenting the need for skepticism as this work continues. Further study of si[$IGLC_{CR}$] must seek to optimize siRNA design, packaging, and delivery for in vivo testing,[50] and this report encourages those ongoing efforts.

Acknowledgments

The authors thank the Division of Hematology-Oncology and Departments of Medicine and Pathology at Tufts for their continued support, Andrew Evens for helpful reading of the manuscript, and the Tufts Medical Center and Tufts University School of Medicine core facilities and their staffs for assistance.

This work was supported by the Amyloidosis and Myeloma Research Fund at Tufts, the Cam Neely and John Davis Myeloma Research Fund, the Sidewater Family Fund, the Lavonne Horowitz Trust, the Werner and Elaine Dannheiser Fund for Research on the Biology of Aging of the Lymphoma Foundation, the Amyloidosis Foundation (P.Z.), and the Demarest Lloyd Jr Foundation, with its continuing commitment to "shutting down the factory" in AL.

Authorship

Contribution: P.Z. and X.M. conceived, designed, and conducted experiments and wrote the manuscript; C.C. conducted clinical research, obtained patient marrows, and wrote the manuscript; L.I. oversaw microarrays, analyzed and presented gene expression studies, and wrote the manuscript; and R.L.C. conceived the design of the research and wrote the manuscript.

Conflict-of-interest disclosure: The authors declare no competing financial interests.

Correspondence: Raymond L. Comenzo, Tufts Medical Center, Box 826, 800 Washington St, Boston, MA 02111; e-mail rcomenzo@tuftsmedicalcenter.org.

References

1. Wechalekar AD, Offer M, Gillmore JD, Hawkins PN, Lachmann HJ. Cardiac amyloidosis, a monoclonal gammopathy and a potentially misleading mutation. *Nat Clin Pract Cardiovasc Med.* 2009;6(2):128-133.
2. Merlini G, Wechalekar AD, Palladini G. Systemic light chain amyloidosis: an update for treating physicians. *Blood.* 2013;121(26):5124-5130.
3. Gertz MA. Immunoglobulin light chain amyloidosis: 2013 update on diagnosis, prognosis, and treatment. *Am J Hematol.* 2013; 88(5):416-425.
4. Cohen AD, Comenzo RL. Systemic light-chain amyloidosis: advances in diagnosis, prognosis, and therapy. *Hematol Am Soc Hematol Educ Program.* 2010;2010(1):287-294.
5. Palladini G, Comenzo RL. The challenge of systemic immunoglobulin light-chain amyloidosis (Al). *Subcell Biochem.* 2012;65:609-642.
6. Iwakoshi NN, Lee AH, Vallabhajosyula P, Otipoby KL, Rajewsky K, Glimcher LH. Plasma cell differentiation and the unfolded protein response intersect at the transcription factor XBP-1. *Nat Immunol.* 2003;4(4):321-329.

7. Feige MJ, Groscurth S, Marcinowski M, et al. An unfolded CH1 domain controls the assembly and secretion of IgG antibodies. *Mol Cell.* 2009;34(5): 569-579.
8. Kim R, Emi M, Tanabe K, Murakami S. Role of the unfolded protein response in cell death. *Apoptosis.* 2006;11(1):5-13.
9. Ryno LM, Wiseman RL, Kelly JW. Targeting unfolded protein response signaling pathways to ameliorate protein misfolding diseases. *Curr Opin Chem Biol.* 2013;17(3): 346-352.
10. Arendt BK, Ramirez-Alvarado M, Sikkink LA, et al. Biologic and genetic characterization of the novel amyloidogenic lambda light chain-secreting human cell lines, ALMC-1 and ALMC-2. *Blood.* 2008;112(5):1931-1941.
11. Zhou P, Hoffman J, Landau H, Hassoun H, Iyer L, Comenzo RL. Clonal plasma cell pathophysiology and clinical features of disease are linked to clonal plasma cell expression of cyclin D1 in systemic light-chain amyloidosis. *Clin Lymphoma Myeloma Leuk.* 2012;12(1):49-58.
12. Comenzo RL, Zhang Y, Martinez C, Osman K, Herrera GA. The tropism of organ involvement in primary systemic amyloidosis: contributions of Ig V(L) germ line gene use and clonal plasma cell burden. *Blood.* 2001;98(3):714-720.
13. Brito JL, Davies FE, Gonzalez D, Morgan GJ. Streptolysin-O reversible permeabilisation is an effective method to transfect siRNAs into myeloma cells. *J Immunol Methods.* 2008; 333(1-2):147-155.
14. Zhou P, Kalakonda N, Comenzo RL. Changes in gene expression profiles of multiple myeloma cells induced by arsenic trioxide (ATO): possible mechanisms to explain ATO resistance in vivo. *Br J Haematol.* 2005;128(5):636-644.
15. Zhou P, Teruya-Feldstein J, Lu P, Fleisher M, Olshen A, Comenzo RL. Calreticulin expression in the clonal plasma cells of patients with systemic light-chain (AL-) amyloidosis is associated with response to high-dose melphalan. *Blood.* 2008; 111(2):549-557.
16. Du P, Kibbe WA, Lin SM. lumi: a pipeline for processing Illumina microarray. *Bioinformatics.* 2008;24(13):1547-1548.
17. Smyth GK. Linear models and empirical Bayes methods for assessing differential expression in microarray experiments. *Stat Appl Genet Mol Biol.* 2004;3(1):Article3.
18. Saeed AI, Bhagabati NK, Braisted JC, et al. TM4 microarray software suite. *Methods Enzymol.* 2006;411:134-193.
19. Huang DW, Sherman BT, Lempicki RA. Systematic and integrative analysis of large gene lists using DAVID bioinformatics resources. *Nat Protoc.* 2009;4(1):44-57.
20. Feng G, Shaw P, Rosen ST, Lin SM, Kibbe WA. Using the bioconductor GeneAnswers package to interpret gene lists. *Methods Mol Biol.* 2012;802: 101-112.
21. Hamilton MS, Ball J, Bromidge E, Lowe J, Franklin IM. Characterization of new IgG lambda myeloma plasma cell line (EJM): a further tool in the investigation of the biology of multiple myeloma. *Br J Haematol.* 1990;75(3):378-384.
22. Cao SS, Kaufman RJ. Unfolded protein response. *Curr Biol.* 2012;22(16):R622-R626.
23. Fribley A, Zhang K, Kaufman RJ. Regulation of apoptosis by the unfolded protein response. *Methods Mol Biol.* 2009;559:191-204.
24. Gomez-Bougie P, Wuillème-Toumi S, Ménoret E, et al. Noxa up-regulation and Mcl-1 cleavage are associated to apoptosis induction by bortezomib in multiple myeloma. *Cancer Res.* 2007;67(11): 5418-5424.
25. Morales AA, Kurtoglu M, Matulis SM, et al. Distribution of Bim determines Mcl-1 dependence or codependence with Bcl-xL/Bcl-2 in Mcl-1-expressing myeloma cells. *Blood.* 2011;118(5): 1329-1339.
26. Lin FR, Huang SY, Hung KH, et al. ASK1 promotes apoptosis of normal and malignant plasma cells. *Blood.* 2012;120(5):1039-1047.
27. Tabas I, Ron D. Integrating the mechanisms of apoptosis induced by endoplasmic reticulum stress. *Nat Cell Biol.* 2011;13(3):184-190.
28. Obeng EA, Carlson LM, Gutman DM, Harrington WJ Jr, Lee KP, Boise LH. Proteasome inhibitors induce a terminal unfolded protein response in multiple myeloma cells. *Blood.* 2006;107(12): 4907-4916.
29. Hetz C. The unfolded protein response: controlling cell fate decisions under ER stress and beyond. *Nat Rev Mol Cell Biol.* 2012;13(2): 89-102.
30. Davenport EL, Morgan GJ, Davies FE. Untangling the unfolded protein response. *Cell Cycle.* 2008; 7(7):865-869.
31. Dong H, Chen L, Chen X, et al. Dysregulation of unfolded protein response partially underlies proapoptotic activity of bortezomib in multiple myeloma cells. *Leuk Lymphoma.* 2009;50(6): 974-984.
32. White-Gilbertson S, Hua Y, Liu B. The role of endoplasmic reticulum stress in maintaining and targeting multiple myeloma: a double-edged sword of adaptation and apoptosis. *Front Genet.* 2013;4:109.
33. Haas IG, Wabl MR. Immunoglobulin heavy chain toxicity in plasma cells is neutralized by fusion to pre-B cells. *Proc Natl Acad Sci USA.* 1984;81(22): 7185-7188.
34. Morris JA, Dorner AJ, Edwards CA, Hendershot LM, Kaufman RJ. Immunoglobulin binding protein (BiP) function is required to protect cells from endoplasmic reticulum stress but is not required for the secretion of selective proteins. *J Biol Chem.* 1997;272(7):4327-4334.
35. Hebert DN, Gierasch LM. The molecular dating game: an antibody heavy chain hangs loose with a chaperone while waiting for its life partner. *Mol Cell.* 2009;34(6):635-636.
36. Corcos D, Osborn MJ, Matheson LS, et al. Immunoglobulin aggregation leading to Russell body formation is prevented by the antibody light chain. *Blood.* 2010;115(2):282-288.
37. Zou X, Piper TA, Smith JA, Allen ND, Xian J, Brüggemann M. Block in development at the pre-B-II to immature B cell stage in mice without Ig kappa and Ig lambda light chain. *J Immunol.* 2003;170(3):1354-1361.
38. Katzmann JA, Clark RJ, Abraham RS, et al. Serum reference intervals and diagnostic ranges for free kappa and free lambda immunoglobulin light chains: relative sensitivity for detection of monoclonal light chains. *Clin Chem.* 2002;48(9): 1437-1444.
39. Magrangeas F, Cormier ML, Descamps G, et al. Light-chain only multiple myeloma is due to the absence of functional (productive) rearrangement of the IgH gene at the DNA level. *Blood.* 2004; 103(10):3869-3875.
40. Kühnemund A, Liebisch P, Bauchmüller K, et al. 'Light-chain escape-multiple myeloma'-an escape phenomenon from plateau phase: report of the largest patient series using LC-monitoring. *J Cancer Res Clin Oncol.* 2009;135(3):477-484.
41. Qu X, Zhang L, Fu W, et al. An infrequent relapse of multiple myeloma predominantly manifesting as light chain escape: clinical experience from two Chinese centers. *Leuk Lymphoma.* 2010;51(10): 1844-1849.
42. Wang Q, Mora-Jensen H, Weniger MA, et al. ERAD inhibitors integrate ER stress with an epigenetic mechanism to activate BH3-only protein NOXA in cancer cells. *Proc Natl Acad Sci USA.* 2009;106(7):2200-2205.
43. Kurata K, Yanagisawa R, Ohira M, Kitagawa M, Nakagawara A, Kamijo T. Stress via p53 pathway causes apoptosis by mitochondrial Noxa upregulation in doxorubicin-treated neuroblastoma cells. *Oncogene.* 2008;27(6): 741-754.
44. Mannava S, Zhuang D, Nair JR, et al. KLF9 is a novel transcriptional regulator of bortezomib- and LBH589-induced apoptosis in multiple myeloma cells. *Blood.* 2012;119(6):1450-1458.
45. Rizzatti EG, Mora-Jensen H, Weniger MA, et al. Noxa mediates bortezomib induced apoptosis in both sensitive and intrinsically resistant mantle cell lymphoma cells and this effect is independent of constitutive activity of the AKT and NF-kappaB pathways. *Leuk Lymphoma.* 2008;49(4):798-808.
46. Coelho T, Adams D, Silva A, et al. Safety and efficacy of RNAi therapy for transthyretin amyloidosis. *N Engl J Med.* 2013;369(9):819-829.
47. Phipps JE, Kestler DP, Foster JS, et al. Inhibition of pathologic immunoglobulin-free light chain production by small interfering RNA molecules. *Exp Hematol.* 2010;38(11):1006-1013.
48. Hovey BM, Ward JE, Soo Hoo P, O'Hara CJ, Connors LH, Seldin DC. Preclinical development of siRNA therapeutics for AL amyloidosis. *Gene Ther.* 2011;18(12):1150-1156.
49. Zhou Y, Chen L, Barlogie B, et al. High-risk myeloma is associated with global elevation of miRNAs and overexpression of EIF2C2/AGO2. *Proc Natl Acad Sci USA.* 2010;107(17): 7904-7909.
50. Zhou J, Tiemann K, Chomchan P, et al. Dual functional BAFF receptor aptamers inhibit ligand-induced proliferation and deliver siRNAs to NHL cells. *Nucleic Acids Res.* 2013;41(7):4266-4283.